Int. J. Electrochem. Sci., 6 **(2011)** 1772 - 1784

International Journal of
ELECTROCHEMICAL
SCIENCE
www.electrochemsci.org

Corrosion Inhibition of Carbon Steel in 0.5M HCl by Monopropianate

R. Lopez-Sesenes[1], *J.G. Gonzalez-Rodriguez*[1,*], *M. Casales*[2], *L. Martinez*[2,3], *J.C. Sanchez-Ghenno*[3,4]

[1] Universidad Autonoma del Estado de Morelos, CIICAp, Av. Universidad 1001, Col. Chamilpa, 62209, Cuernavaca, Mor., Mexico
[2] Universidad Nacional Autonoma de Mexico, Instituto de Ciencias Fisicas Av. Universidad s/n, Col. Chamilpa, 62209, Cuernavaca, Mor., Mexico
[3] Corrosion y Proteccion A.C., Rio Nasas, Cuernavaca,Mor., Mexico
[4] PEMEX DCO. Torre Ejecutiva, Marina Nacional 329, Col. Huasteca, 11311-Mexico, D.F.,Mexico.
[*]E-mail: ggonzalez@uaem.mx

Received: 9 February 2011 / *Accepted:* 5 May 2011 / *Published:* 1 June 2011

A study of monopropianate (N-Coco alkyl aminopropionic acid) as a corrosion inhibitor for carbon steel in 0.5M HCl has been carried out by using weight loss and electrochemical tests, namely potentiodynamic polarization curves and electrochemical impedance spectroscopy at 25, 40 and 60°C. Results have shown that monopropianate is a good inhibitor for the corrosion of 1018 carbon steel in this acidic environment. Inhibitor efficiency increases with increasing the inhibitor concentration but decreases with an increase in the testing temperature. Inhibitor efficiency increases with time at 25 °C but at higher temperatures it decreases. This is explained in terms of corrosion process control and inhibitor adsorption isotherm.

Keywords: Carbon steel, corrosion inhibitor, hydrochloric acid

1. INTRODUCTION

Aggressive acid solutions are widely used for industrial purposes, such as chemical, acid de-scaling and pickling processes to remove corrosion scales from the metallic surface in highly concentrated hydrochloric acid at elevated temperature up to 60°C. The use of inhibitors is one of the most practical methods to protect metals against acid attack. Most widely used acid inhibitors are organic compounds containing oxygen, nitrogen and/or sulfur [1-5]. Acid inhibitors have many important roles in the industrial field such as a component in pre-treatment composition, cleaning

solutions and in acidification of oil wells. Hetero-atoms as sulfur, phosphorus, nitrogen and oxygen as well as aromatic rings in their structure are the major adsorption centers.

Some works have studied the influence of organic compounds containing nitrogen on the corrosion resistance of steel in acidic media [6-18] most organic inhibitors acting by adsorption on the metal surface. To be effective, an inhibitor must be also displace water from the metals surface, to block active corrosion sites and interact with the anodic or cathodic reaction sites to retard the oxidation and/or reduction of corrosion reaction. So, the inhibition efficiency of organic compounds depends on the structure of the inhibitor, the characteristics of the environment, etc….Several organic compounds have been evaluated as corrosion inhibitors for carbon steel in acidic media [6-18], so, the aim of this work is to study the inhibition properties of monopropianate (N-Coco alkyl aminopropionic acid) for the corrosion of 1018 carbon steel in 0.5M HCl. Two main techniques were employed: chemical (weight loss) and electrochemical (potentiodynamic and electrochemical impedance spectroscopy, EIS).

2. EXPERIMENTAL

2.1. Test material

The experiments were performed with 1018 type carbon steel specimens. Cylindrical specimens with an exposed area of 1.0 cm^2 were encapsulated in epoxy resin. Before each test the electrodes were polished to 600 emery paper and then cleaned with distilled water, alcohol, and finally acetone.

2.2. Test solution

The aggressive solutions used were made of AR grade 37% HCl. A 0.5M HCl solution was prepared by using distilled water. The concentrations range of inhibitor employed was 5-100 ppm. The organic inhibitor used has the structure given on Fig. 1 which was dissolved in pure 2-propanol.

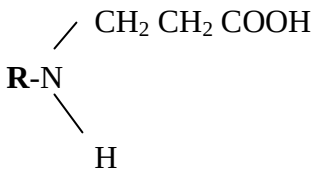

Figure 1. General structure of monopropianate, C12/C14, where R is an alkyl group.

2.3. Gravimetric measurements.

Weight loss test were obtained in a glass cell with coupons which were 2.0 cm long, 1.0 cm wide and 0.5 cm thick abraded with 600 grade emery paper. Then, the specimens were washed several

times with distilled water then with acetone and dried using a stream of hot air. After weighing accurately, the specimens were immersed in 100 ml beaker, which contained 100 ml of 0.5M HCl with and without inhibitor at different concentrations. All the aggressive solutions were open to air. After a total time of exposition of 72 hours, specimens were taken out, washed, dried and weighed accurately. Tests were performed by triplicate at room temperature (25°C), 40 and 60°C by using a hot plate. Corrosion rates, in terms of weight loss measurements, $\Delta\omega$, were calculated as follows:

$$\Delta\omega = (m_1 - m_2)/ A \quad [1]$$

were m_1 is the mass of the specimen before corrosion, m_2 the mass of the specimen after corrosion, and A the exposed area of the specimen. For the weight loss tests, inhibitor efficiency, η, was calculated as follows:

$$\eta\ (\%) = 100\ (\Delta\omega_1 - \Delta\omega_2)/ \Delta\omega_1 \quad [2]$$

were $\Delta\omega_1$ is the weight loss without inhibitor, and $\Delta\omega_2$ the weight loss with inhibitor.

2.4. Electrochemical measurements

Electrochemical techniques employed included potentiodynamic polarization curves and electrochemical impedance spectroscopy measurements, EIS. Polarization curves were recorded at a constant sweep rate of 1 mV/s at the interval from -500 to +500 mV respect to the open circuit potential, E_{corr}. Measurements were obtained by using a conventional three electrodes glass cell with two graphite electrodes symmetrically distributed and a saturated calomel electrode (SCE) as reference with a Lugging capillary bridge. Corrosion current density values, I_{corr}, were obtained by using Tafel extrapolation. Electrochemical impedance spectroscopy tests were carried out at E_{corr} by using a signal with amplitude of 10 mV in a frequency interval of 100 mHz-100KHz. An ACM potentiostat controlled by a desk top computer was used for the polarization curves, whereas for the EIS measurements, a model PC4 300 Gamry potentiostat was used. Tests were conducted at room temperature (25°C), 40 and 60°C.

3. RESULTS AND DISCUSSION

Table 1 shows the effect of inhibitor concentration and temperature tests on the inhibitor efficiency for 1018 carbon steel in 0.5M HCl. This table shows that, for a given temperature, inhibitor efficiency increases with the inhibitor concentration, reaching its highest value of 85.4% with an inhibitor concentration of 100 ppm. Table 1 also indicates that even at as low concentrations as 5 ppm of monopropianate gave 30.5% protection to 1018 carbon steel in 0.5M HCl at 25°C, and with 50 ppm concentration, its protection was higher than 50%. Additionally, at a given inhibitor concentration, inhibitor efficiency decreases with increasing the temperature, which suggests that the corrosion

inhibition might be caused by the inhibitor adsorption onto the steel surface from the acidic solution, and higher temperatures might cause the desorption of the inhibitor from the steel surface.

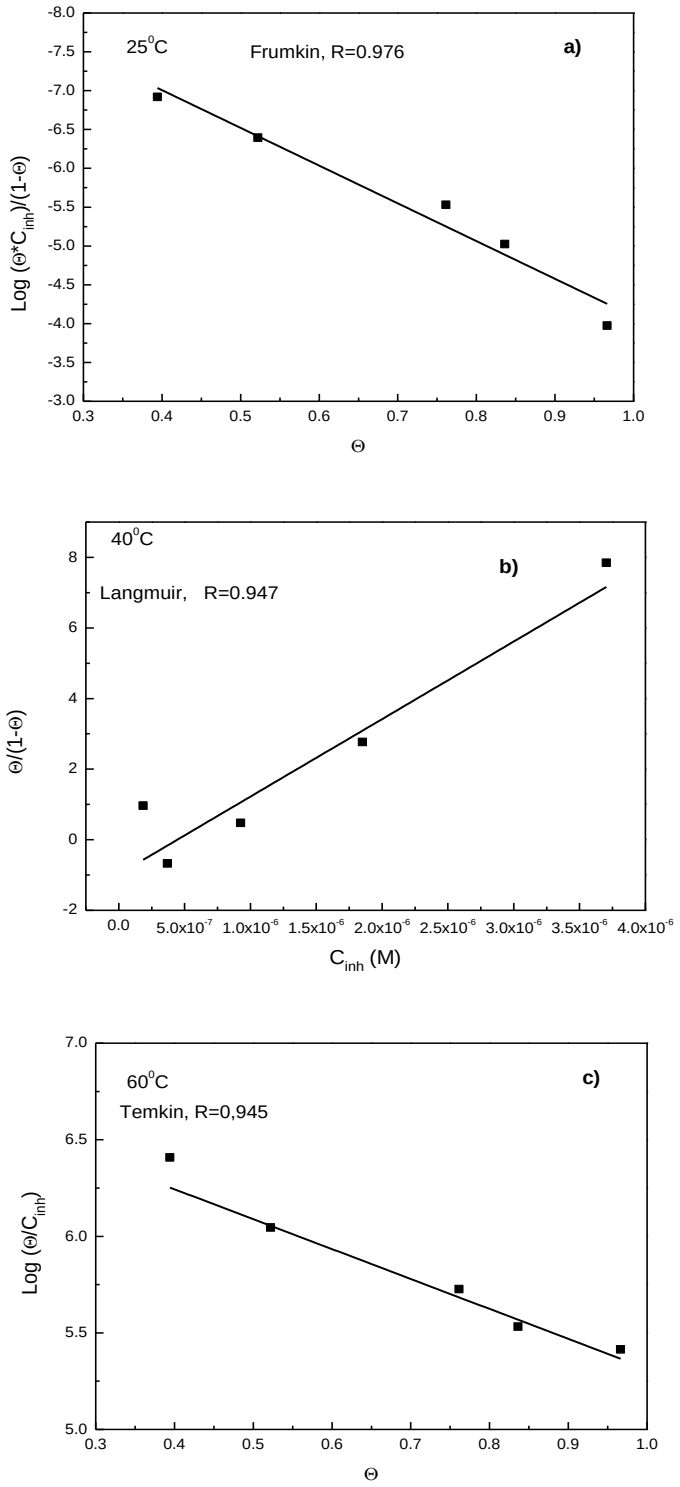

Figure 2. Adsorption isotherms for monopropianate on 1018 carbon steel in 0.5M HCl at a) 25, b) 40 and c) 60°C.

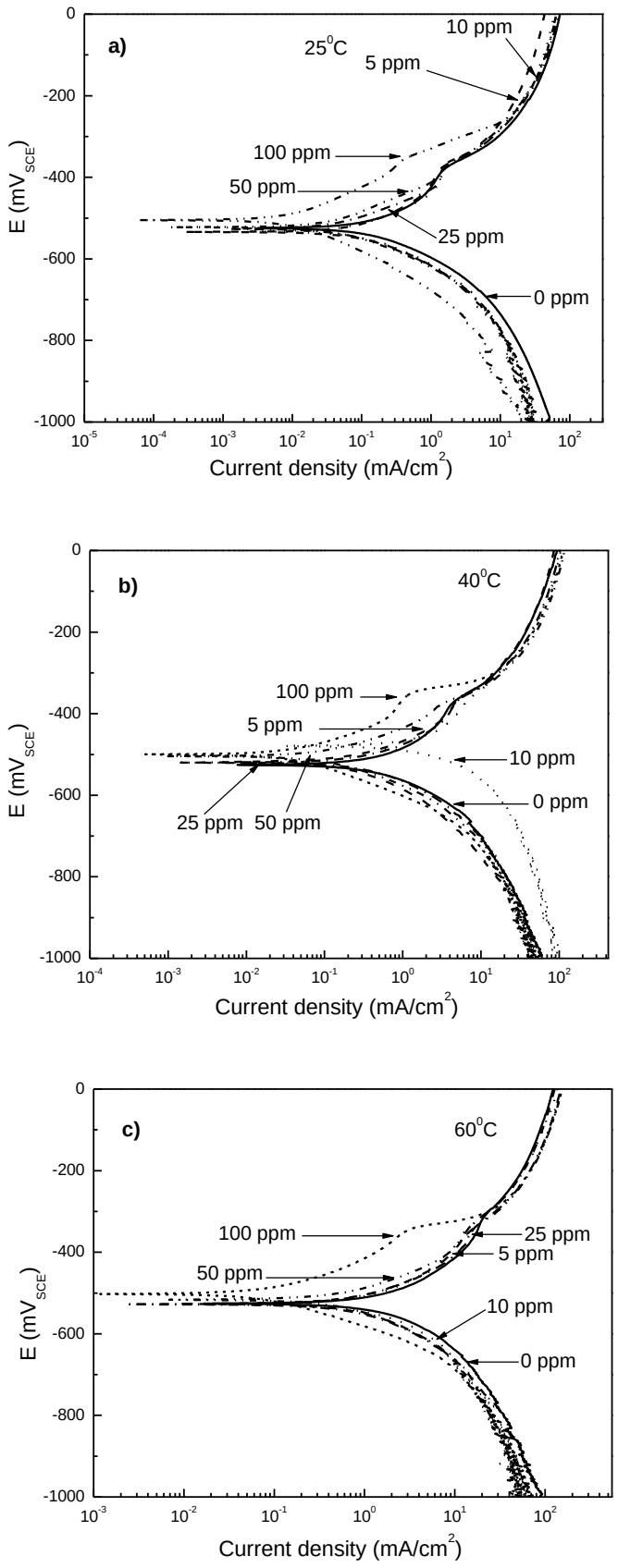

Figure 3. Effect of monopropianate concentration in the polarization curves for 1018 carbon steel in 0.5M HCl at a) 25, b) 40 and c) 60°C.

Table 1. Effect of monopropianate concentration on the inhibitor efficiency at different testing temperatures.

Inhibitor concentration (ppm)	Inhibitor efficiency (%)		
	25°C	40°C	60°C
5	30.5	7.7	3.3
10	40	15.7	9.1
25	44	21.3	14.5
50	54.7	32.1	17.6
100	85.4	66.7	23.3

Assuming the corrosion inhibition was caused by the adsorption of inhibitor, and the degree of surface coverage, Θ, for different concentrations of inhibitor in 0.5M HCl was evaluated from weight loss measurements using equation:

$$\Theta = \eta/100 \qquad [3]$$

From the values of η shown on table 1, it can be seen that Θ increases with increasing inhibitor concentration as a result of more inhibitor molecules being adsorbed on the steel surface when the inhibitor concentration was increased. Now, assuming the adsorption of inhibitor belonged to monolayer adsorption, different adsorption isotherms, namely Langmuir, Temkin, Frumkin and Flory–Huggins, were applied. Fig. 2 shows that at 25°C a Frumkin adsorption isotherm had the best fitting, at 40°C a Langmuir adsorption isotherm was applied, whereas, the best fitting for the adsorption isotherms at 60°C was obtained with a Temkin type of interaction.

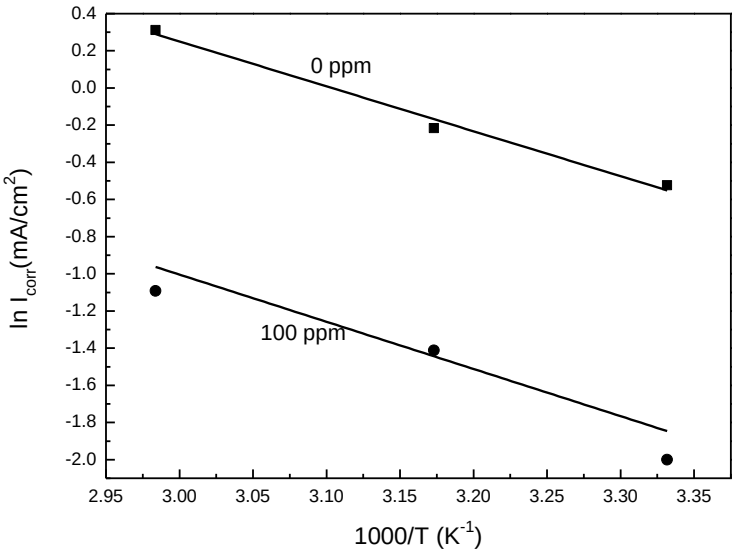

Figure 4. Arrhenius plots of the I_{corr} values for 1018 carbon steel in 0.5M HCl and in 0.5M HCl + 100 ppm of monopropianate.

Polarization curves for 1018 carbon steel in 0.5M HCl at different inhibitor concentrations and temperatures are shown in Fig. 3. It can be seen that, at 25°C, Fig. 3 a, both anodic and cathodic current density values are lowered, thus, this inhibitor is a mixed type of inhibitor. The corrosion current density is decreased and the free corrosion potential value, E_{corr}, is made nobler as the inhibitor concentration increases. At 40 and 60°C, Fig. 3 b and c, the effect of the inhibitor was the same as that at 25°C, decreasing both the anodic and cathodic current density values, but the I_{corr} observed increased as the temperature was increased. It has to be noted that, in all cases, the slope of the cathodic branch for all inhibitor concentrations was nearly equal, indicating that the hydrogen evolution controlled and the proton discharge mechanism reaction did not change by the addition of the inhibitor to the 0.5M HCl solution.

Fig. 4 shows the Arrhenius plots of the corrosion current density. The apparent activation energies can be determined from the relation:

$$I_{corr} = K \exp(-E_a/RT) \qquad [4]$$

where E_a is the apparent activation energy, R the gas constant, T the absolute temperature and K is a constant. The values of the apparent activation energy were 21.1 and 20.1 kJ mol^{-1} with and without inhibitor respectively.

EIS data in both Nyquist and Bode formats for the different inhibitor concentrations at 25°C are shown in Fig. 5. It can be seen that Nyquist diagrams, Fig. 5 a, show in all cases a single capacitive-like semicircle with its center in the real axis, indicating that the corrosion process is under charge transfer control. The semicircle diameter, which represents the double electrochemical layer resistance, R_{ct}, and is inversely proportional to the corrosion current density I_{corr}, increases as the inhibitor concentration increases, indicating that the corrosion rate decreases with the inhibitor concentration, in accordance to the weight loss tests and polarization curves.

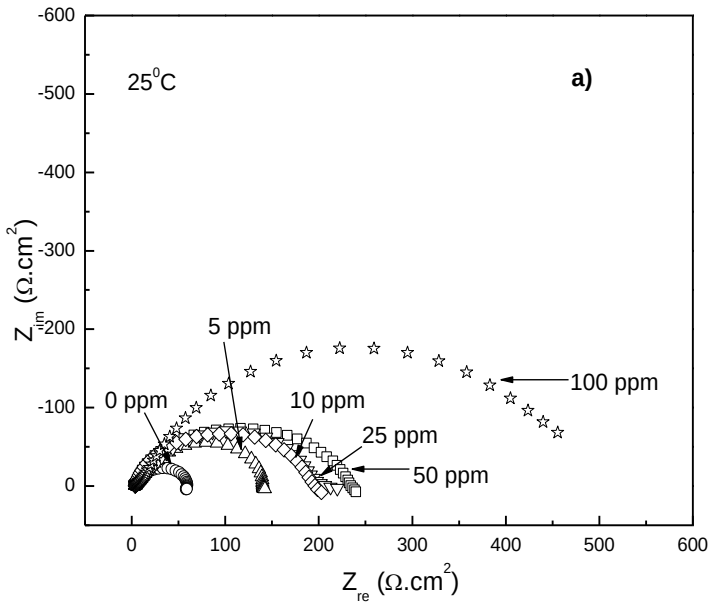

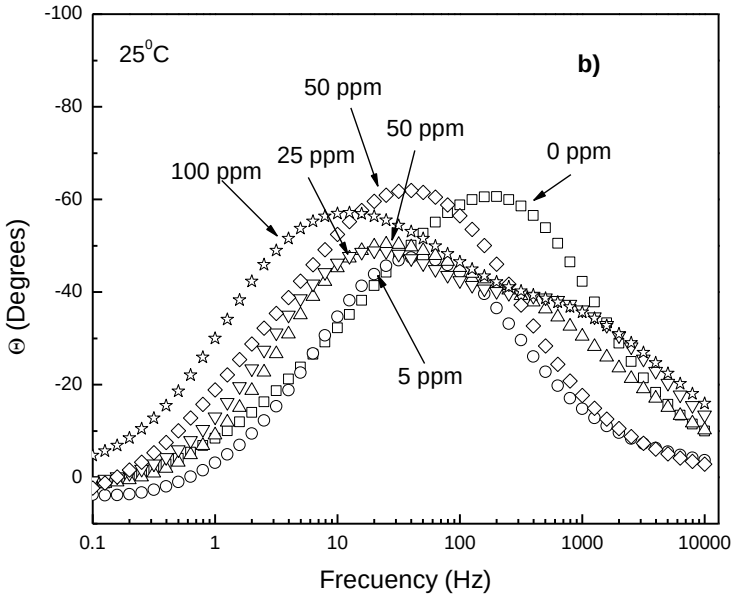

Figure 5. EIS data in the a) Nyquist and b) Bode format for 1018 carbon steel in uninhibited and inhibited 0.5M HCl solution at 25°C.

Bode diagrams, Fig. 5 b, show one peak only at lower inhibitor doses lower than 10 ppm, indicating the absence of any protective film at these inhibitor concentrations. However, for inhibitor concentrations higher than 25 ppm, two peaks are found at 10 and 1000 Hz, indicating the formation of a protective film-formed inhibitor under these conditions.

The EIS data for 1018 carbon steel in 0.5M HCl at 40°C are shown in Fig. 6. Nyquist diagrams, Fig. 6 a, show a single capacitive-like semicircle at intermediate and high frequency values, but at lower frequencies, the presence of a smaller inductive loop are evident.

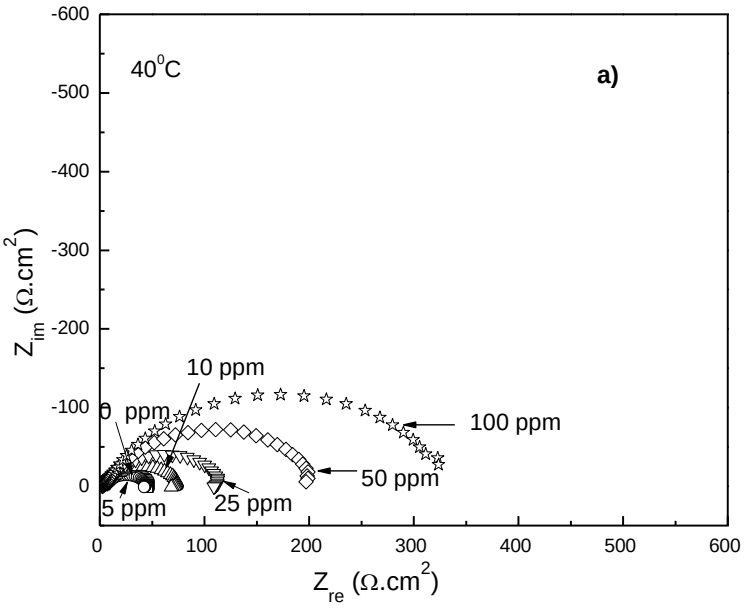

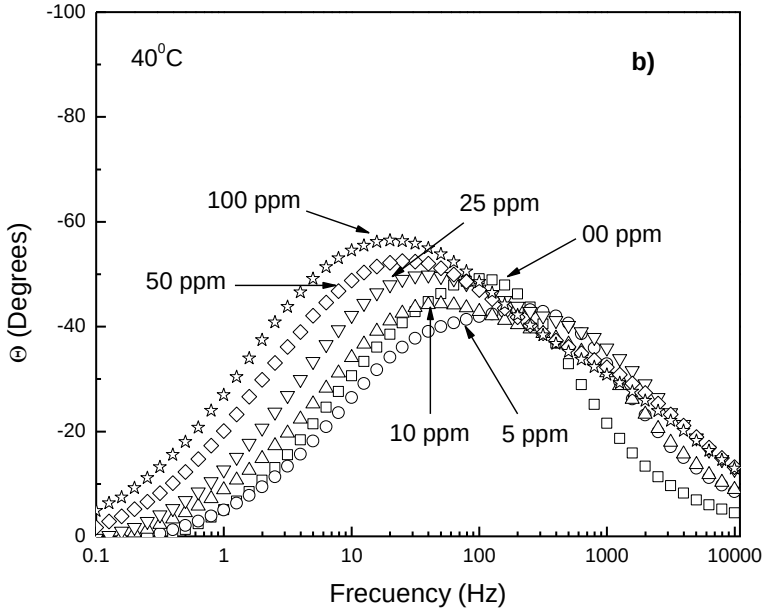

Figure 6. EIS data in the a) Nyquist and b) Bode format for 1018 carbon steel in uninhibited and inhibited 0.5M HCl solution at 40°C.

This loop indicates that the corrosion process is under the control of the adsorption of the inhibitor or a complex formed by the inhibitor and the corrosion products. The semicircle diameter increases with the inhibitor concentration, showing a decrease of the corrosion rate. However, the semicircle diameters at 40°C are smaller than those obtained at 25°C, indicating an increase in the corrosion rate at 40°C. Bode diagrams, Fig. 6 b, show one peak only at low inhibitor concentrations, indicating the absence of a protective film. However, for inhibitor concentration higher than 25 ppm, there appear two peaks, indicating the presence of a protective film-formed inhibitor, which explains the decrease in the corrosion rate as the inhibitor doses increases.

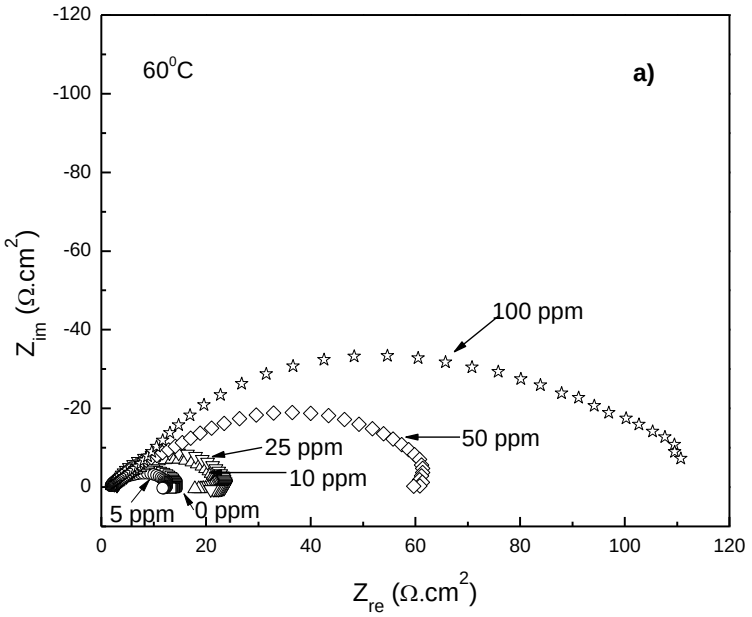

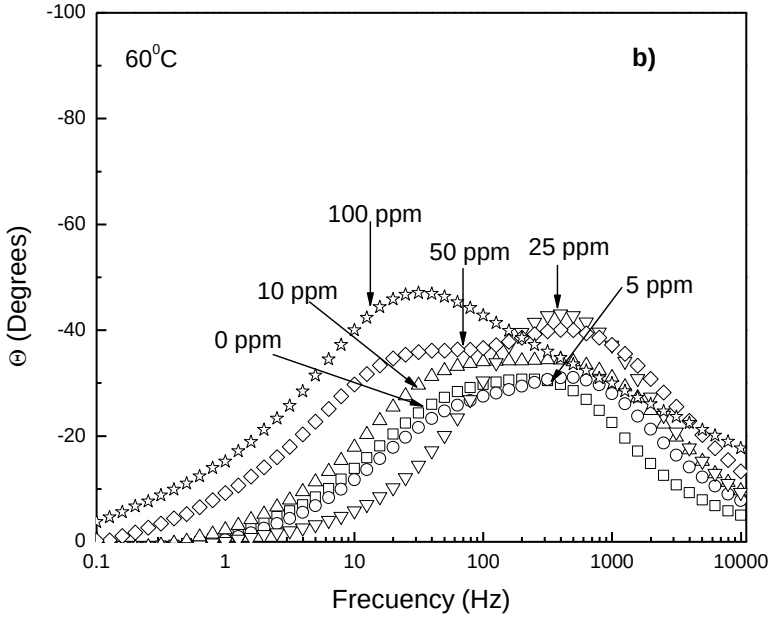

Figure 7. EIS data in the a) Nyquist and b) Bode format for 1018 carbon steel in uninhibited and inhibited 0.5M HCl solution at 60°C.

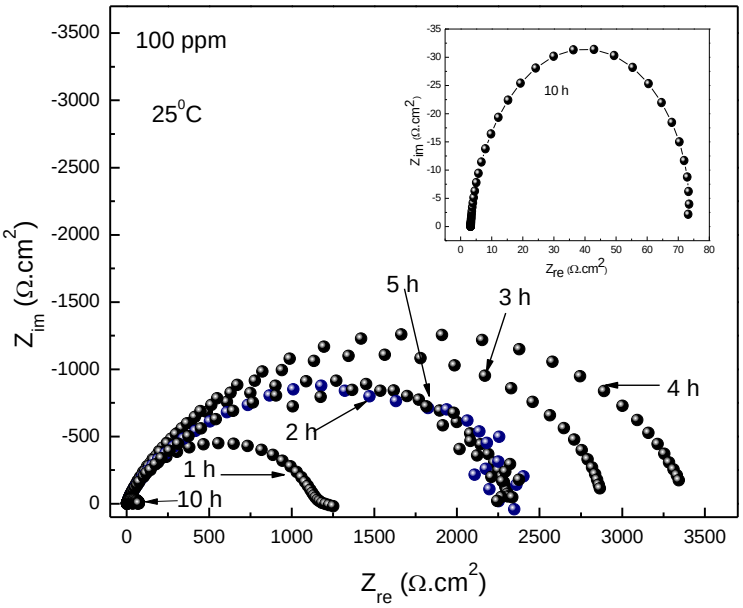

Figure 8. Nyquist diagrams for 1018 carbon steel corroded in 0.5M HCl + 100 ppm of monopropianate at 25°C at different exposure times.

At 60°C, Fig. 7 a, Nyquist diagrams show similar features to those found at 40°C, with a single capacitive-like semicircle at intermediate and high frequency values, but the presence of a small inductive loop at lower frequencies is much more evident than at 40°C. However, the semicircle diameters, which increased with the inhibitor concentration, are much smaller than those found at lower temperatures, confirming the above results which showed an increase in the corrosion rate with

an increase in the testing temperature. Bode diagrams, Fig. 7 b, show, once again, one peak only al low inhibitor concentrations and two peaks at high doses. However, the phases for the tests at 60°C are lower than those at 25 and 40°C due, probably, to the increase in the corrosion rate with an increase in the temperature.

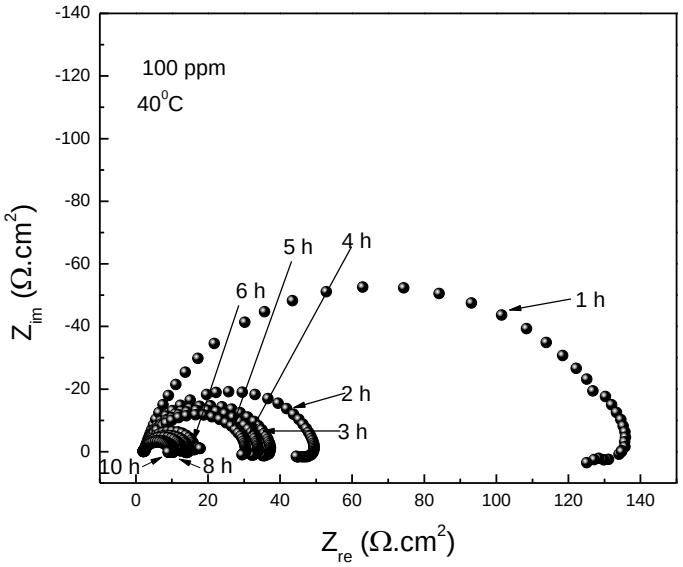

Figure 9. Nyquist diagrams for 1018 carbon steel corroded in 0.5M HCl + 100 ppm of monopropianate at 40°C at different exposure times.

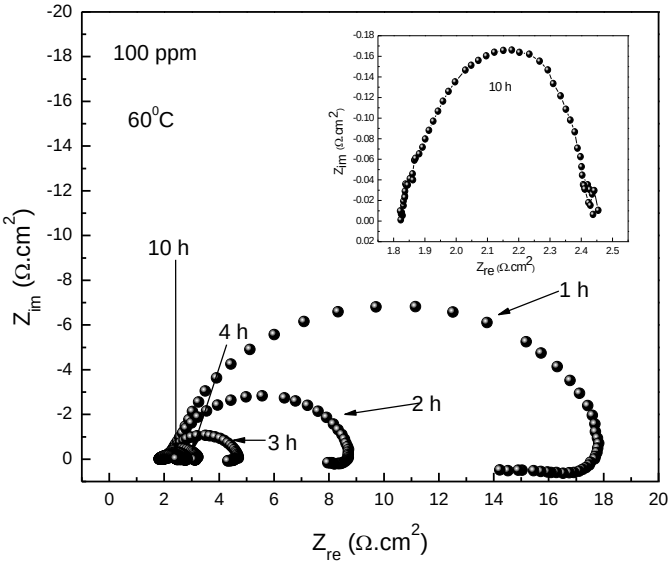

Figure 10. Nyquist diagrams for 1018 carbon steel corroded in 0.5M HCl + 100 ppm of monopropianate at 60°C at different exposure times.

To have an insight on the film-formed inhibitor stability, some longer tests were performed at the inhibitor concentration where the lowest corrosion rate was found, i.e. 100 ppm, at the different

tested temperatures. Fig. 8 shows Nyquist diagrams for 1018 carbon steel immersed in 0.5 M HCl with 100 ppm of inhibitor at 25°C at different immersion times. It can be seen that in all cases, data describe a single capacitive semicircle, with its diameter increasing with time up to 4 hours, indicating a decrease in the corrosion rate and showing that the film-formed inhibitor increases its protectiveness. However, for longer times than 4 hours, the semicircle diameter decreases, indicating an increase in the corrosion rate as time elapses, and that the film protectiveness decreases, maybe because under these conditions the protective film is desorbed from metal surface. However, at 40 and 60°C, Figs. 9-10, the evidence of an inductive loop at low frequencies is more evident, since at 25°C it was absent, but now the semicircle diameter increases with time, indicating a decrease in the corrosion rate as time elapses since the beginning of the experiment, which shows that, at these temperatures, the film-formed inhibitor is very unstable and is easily desorbed from metal surface or dissolved by the environment. It should be noted that the semicircle diameter decreases with increasing the temperature for more than two orders of magnitude, showing that at room temperature this inhibitor improves its performance as time elapses, during the first 4 hours. However, at 40 and 60°C the inhibitor performance decreases considerably.

All data have shown that inhibitor efficiency increases with increasing the inhibitor concentration but decreases with the temperature. In addition, Nyquist diagrams have shown that at 25°C the corrosion process is under charge transfer control from the steel surface to the environment through the double electrochemical layer, but at 40 and 60°C, the corrosion process is under the control of adsorption-desorption of some species or inhibitor-formed film. Also, adsorption isotherms have shown three different kind of isotherms depending upon the working temperature: Frumklin at 25, Langmuir at 40 and Temkin at 60°C. Langmuir isotherm considers uniform activity over the surface for adsorption to take place and no interaction among adsorbed molecules. Frumkin and Temkin consider a lateral interaction between adsorbed inhibitor molecules. Thus, the adsorption mechanism at 25°C considers lateral interaction among inhibitor and water molecules, indicating that the inhibitor is displacing water molecules from the steel surface; at 60°C there is lateral interaction between inhibitor molecules and corrosion products which displace inhibitor molecules, leading to a inhibitor desorption and an increase in the corrosion rate as compared with that at lower temperatures, decreasing inhibitor efficiency.

4. CONCLUSIONS

A study of monopropianate (N-coco alkyl aminopropionic acid) as a corrosion inhibitor for carbon steel in 0.5M HCl has been carried out by using weight loss and electrochemical tests. Results have shown that monopropianate is a good inhibitor for the corrosion of 1018 carbon steel in this acidic environment. Inhibitor efficiency increases with increasing the inhibitor concentration but decreases with an increase of the testing temperature. At 25°C, inhibitor efficiency increases with time reaching its maximum efficiency at 4 hours, but after this time the inhibitor efficiency decreases with time. At higher temperatures, inhibitor efficiency decreases wit time. This is because at 25°C monopropianate follows a Frumkin type of adsorption isotherm and the corrosion process is under

charge transfer control. At higher temperatures, inhibitor follows two different adsorption isotherms, Lanmuir and Temkin for 40 and 60°C respectively, and the corrosion process is under adsorption-desorption species control.

References

1. M. Elayyachy, M. Elkodadi, A. Aouniti, A. Ramdani, *Mater. Chem. Phys.* 93 (2005) 281-285.
2. A.Popova, M. Christov, S: Raicheva, E. Sokolova, *Corros. Sci*. 46 (2004) 1333-1350.
3. B. Mernari, H. Elatarri, M. Traisnel, F. Bentiss, M. Larenée, *Corros, Sci*. 40 (1998) 391-407.
4. X. Li, S.Deng, H. Fu, T. Li, G. Mu, *Anti-Corr. Methods Mater.* 56 (2009) 232-238.
5. Y.I. Sürme, A. A. Gürten, Corros. *Eng. Sci. Technol*. 44 (2009) 304-3011.
6. G.Y. Elewady, *Int. J. Electrochem. Sci.* 3 (2008) 1149-1161
7. I. Zaafarany, M. Abdallah, *Int. J. Electrochem. Sci.* 5 (2010) 18-28.
8. A.Yurt, A. Balaban, S. Ustün Kandemir, G. Bereket, *Mat. Chem. Phys*. 85 (2004) 420-426.
9. S.A. Ali, H.A. Al-Muallema, S.U. Rahman, M.T. Saeed, *Corros. Sci*. 50 (2008) 3070-3077.
10. H. Ju, Z.P. Kai, Y. Li, *Corros. Sci*. 50 (2008) 865-871.
11. D.I. Gopi, K. Govindaraju, L. Kavhith, *J. Appl. Electrochem*. 40 (2010) 1349-1356.
12. M.A. Migahed, A.M. Abdul-Raheim, A.M. Atta, W. Brostow, *Mat. Chem. Phys*. 121 (2010) 208-214.
13. A.Singh, M. Quraish, *J. Appl. Electrochem*. 40 (2010) 1293-1306.
14. I.B. Obot, N.O. Obi-Egbedi, N.W. Odozi, *Corros. Sci.* 52 (2010) 923-926.
15. I.B. Obot, N.O. Obi-Egbedi, Mater. *Chem. Phys*. 122 (2010) 325-328.
16. H. Ashassi-Sorkhabi, M. Es´haghi, *J. Solid State Electrochem*. 13 (2009) 1297-1301.
17. F.M. Mahgoub, B.A. Abdel-Nabey, Y.A. El-Samadisy, *Mater. Chem. Phys*. 120 (2010) 104-108.
18. B.I. Zerg, M. Sfair, M. Tale, B. Hammouti, M. E. Touhami, S. Radi, Z. Rais, *J. Appl. Electrochem*. 40 (2010) 1575-1582.
19. N.O. Eddy, E.E. Ebenso, *Pigment and Resin Technol*. 39 (2010) 77-83.
20. K.C. Emeregül, A. Abdülkadir Akay, O. Atakol, *Mater. Chem. Phys*. 93 (2005) 325-329.